Arabian Journal of Chemistry (2012) 5, 447–452

King Saud University

Arabian Journal of Chemistry

www.ksu.edu.sa
www.sciencedirect.com

ORIGINAL ARTICLE

1st Nano Update

Solar active nano-TiO_2 for mineralization of Reactive Red 120 and Trypan Blue

R. Velmurugan [a], B. Krishnakumar [a], Rajendra Kumar [b], M. Swaminathan [a,*]

[a] Department of Chemistry, Annamalai University, Annamalainagar 608 002, India
[b] Ministry of Environment and Forest, Paryavaran Bhawan, CGO Complex, Lodhi Road, New Delhi 110 003, India

Received 12 October 2010; accepted 23 December 2010
Available online 29 December 2010

KEYWORDS

Anatase phase nano-TiO_2;
Photocatalysis;
Solar light;
Reactive Red 120;
Trypan Blue

Abstract Nano-TiO_2 was synthesized by sol–gel method. The catalyst was characterized by X-ray diffraction (XRD), scanning electron microscope (SEM) images, transmission electron microscope (TEM), BET surface area measurement and DRS analysis. The formation of anatase phase nano-TiO_2 was confirmed by XRD measurements and its crystalline size is found to be 15.2 nm. SEM images depict the crystalline nature of prepared TiO_2. The BET surface area of prepared TiO_2 is found to be 86.5 $m^2 g^{-1}$ which is higher than that of commercially available TiO_2–P25. The photocatalytic activity of prepared anatase phase TiO_2 has been tested for the degradation of two azo dyes: Reactive Red 120 (RR 120) and Trypan Blue (TB) using solar light. The photocatalytic activity of nano-TiO_2 is higher than TiO_2–P25 under solar light. The mineralization of dyes has been confirmed by chemical oxygen demand (COD) measurements.

1. Introduction

Reactive azo dyes are widely used in the textile industries because of their simple dying procedures and good stability during washing process. But the main drawback of these dyes is low fixation rate on the fabrics. Hence dye wastewater introduces intense color and toxicity to aquatic system. Due to the complex structure and stability of the dyes, conventional biological treatment methods are ineffective for degradation (Huang et al., 1979; Pagga and Brown, 1986; Ince and Gonenc, 1997).

Heterogeneous photocatalysis has been considered as a cost-effective alternative as pre- or post-treatment of biolog-

* Corresponding author. Tel./fax: +91 4144 225072.
E-mail address: chemres50@gmail.com (M. Swaminathan).

Peer review under responsibility of King Saud University.
doi:10.1016/j.arabjc.2010.12.023

Production and hosting by Elsevier

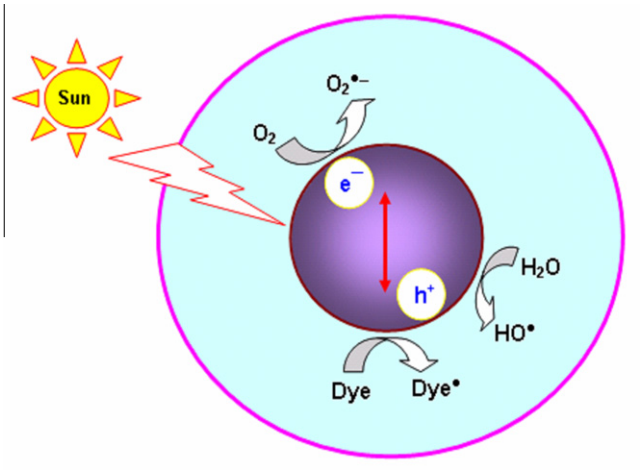

Scheme 1 Electron–hole pair generation in an illuminated semiconductor particle with solar light.

ical treatment process for the purification of dye-containing wastewater (Collins et al., 1978; Luthy and Talton, 1980; Kiwi et al., 1993; Tanaka and Ichikawa, 1993; Wang, 2000). Heterogeneous photocatalysis is based on the irradiation of a photocatalyst, usually a semiconductor such as TiO_2, with light energy equal to or greater than the band gap energy. This causes a valence-band electron to be excited to the conduction band, causing charge separation (Scheme 1). The conduction band electrons and valence band holes can then migrate to the surface and participate in interfacial oxidation–reduction reactions. The oxidative degradation of an organic pollutant is attributed to indirect reaction of positive hole at the surface where adsorbed water or hydroxyl groups are oxidized to hydroxyl radicals ($OH^{\cdot}$), which then react with the pollutant molecule (Turchi and Ollis, 1990). Recently, much attention has been paid to the photocatalytic degradation of dyes with TiO_2 particles under UV or visible light (Toor et al., 2006; Aarthi et al., 2007). We have reported photodegradation of a number of toxic chemicals with commercial ZnO and TiO_2 using UV and solar light (Sobana and Swaminathan, 2007; Muruganandham and Swaminathan, 2006; Ravichandran et al., 2007; Krishnakumar and Swaminathan, 2010). The present work focuses on the preparation and characterization of nano sized TiO_2 and its photocatalytic activity on the degradation of RR 120 and TB with solar light.

2. Experimental

2.1. Materials

The commercial azo dyes, Trypan Blue (Fig. 1a), from SD Fine and Reactive Red 120 (Fig. 1b), from Balaji Colour Company, Dyes and Auxiliaries (Chennai) were used as such. A gift sample of TiO_2–P25 was received from Degussa (Germany). It is a mixture of 80% anatase and 20% rutile with the particle size of 30 nm and BET specific area 50 $m^2 g^{-1}$. AnalaR grade tetraisopropyl orthotitanate (Himedia, 98.0%), isopropanol (99.5%, Spectrochem) were used as received. The double distilled water was used to prepare experimental solutions.

2.2. Preparation of nano-TiO_2

Nano-TiO_2 was prepared by sol–gel method. 12.5 mL of tetraisopropyl orthotitanate was dissolved in 100 mL of isopropanol (Spectrochem $\geqslant$99.5%) and to this solution 3 mL of water was added drop wise under vigorous stirring. The resulting colloidal suspension was stirred for 4 h. The gel obtained was filtered, washed and dried in an air oven at 100 °C for 5 h. The sample was calcinated at 400 °C in a muffle furnace for 12 h.

2.3. Irradiation procedure

Solar photocatalytic degradation experiments were carried out under similar conditions on sunny days between 11 am to 2 pm in the month of May, 2010. An open borosilicate glass tube of 50 mL capacity, 40 cm height and 12.6 mm diameter was used as the reaction vessel. Fifty milliliters of RR 120 (2×10^{-4} M) or TB (1×10^{-4} M) with the appropriate amount of catalyst was stirred for 30 min in the dark prior to illumination in order to achieve maximum adsorption of dye onto the semiconductor surface. Irradiation was carried out in the open air with continuous aeration by a pump to provide oxygen and for the complete mixing of reaction solution. During the illumination time no volatility of the solvent was observed. In all cases, 50 mL of reaction mixture was irradiated. At specific time intervals, 2–3 mL of the sample was withdrawn and centrifuged to separate the catalyst. One milliliter of the sample was suitably diluted and dye concentration was determined from the absorbance at the analytical wavelength (RR 120–285 nm, TB −313 nm).

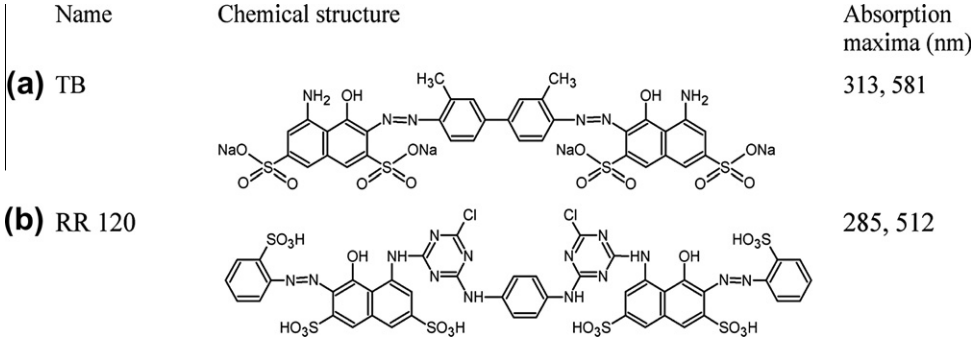

Figure 1 The chemical structures and absorption maxima of (a) TB and (b) RR 120.

2.4. Solar light intensity measurements

Solar light intensity was measured for every 30 min and the average light intensity over the duration of each experiment was calculated. The sensor was always set in the position of maximum intensity. The intensity of solar light was measured using LT Lutron LX-10/A Digital Lux meter and the intensity was 1250×100 lux. The intensity was nearly constant during the experiments.

2.5. Chemical oxygen demand (COD) measurements

COD was determined using the following procedure. Sample was refluxed with $HgSO_4$, known volume of standard $K_2Cr_2O_7$, $AgSO_4$ and H_2SO_4 for two hours and titrated with standard Ferrous Ammonium Sulfate (FAS) using ferroin indicator. A blank titration was carried out with distilled water instead of dye sample. COD was determined using the following equation

$$\text{COD} = \frac{(\text{blank titre value} - \text{dye sample titre value}) \times \text{normality of FAS} \times 8 \times 1000}{\text{Volume of sample}} \quad (1)$$

2.6. Analytical methods

The specific surface area of the catalyst was determined through nitrogen adsorption at 77 K on the basis of BET equation using a micrometrics ASAP 2020 V3.00 H. Scanning electron microscope (SEM) images were taken on gold coated samples using a JEOL-JSM 5610 LV, equipped with OXFORD energy dispersive spectroscopy (EDS). The grids were dried under natural conditions and examined using a TEM Hitachi H-7500. Powder X-ray diffraction patterns of TiO_2 and TiO_2–P25 catalyst were obtained using X'Per PRO diffractometer equipped with a Cu Kα radiation (wavelength 1.5406 Å) at 2.2 kW Max. Peak positions were compared with the standard files to identity the crystalline phase. Avatar-330 FT-IR spectrophotometer was used for recording IR spectra. Diffuse reflectance spectra were recorded using Shimadzu UV-2450. UV spectral measurements were done using Hitachi-U-2001 spectrometer. The pH of the solution was measured by ELICO (LI-10T model) digital pH meter.

3. Results and discussion

3.1. Characterization of catalyst

Prepared TiO_2 was characterized by XRD, SEM, TEM, BET surface area and DRS analysis. XRD pattern of TiO_2–P25 and prepared TiO_2 are given in Fig. 2a and b, respectively. All the marked diffraction peaks of prepared TiO_2 in Fig. 2b can coincidently be indexed by the known anatase phase TiO_2. Characteristic peaks of TiO_2 at 25.3, 37.8, 48.0, 53.9, 54.9, 62.7, 68.7, 69.7 and 75.1 corresponds to (1 0 1), (1 1 2), (2 0 0), (1 0 5), (2 1 1), (2 0 4), (1 1 6), (2 2 0) and (2 1 5) diffraction peaks of anatase phase TiO_2. Fig. 2a displays the XRD pattern of Degussa TiO_2–P25 since it is a mixture of 80% anatase and 20% rutile XRD pattern shows both anatase and rutile lines. The crystalline size of prepared TiO_2 was determined using the following Debye–Scherrer equation:

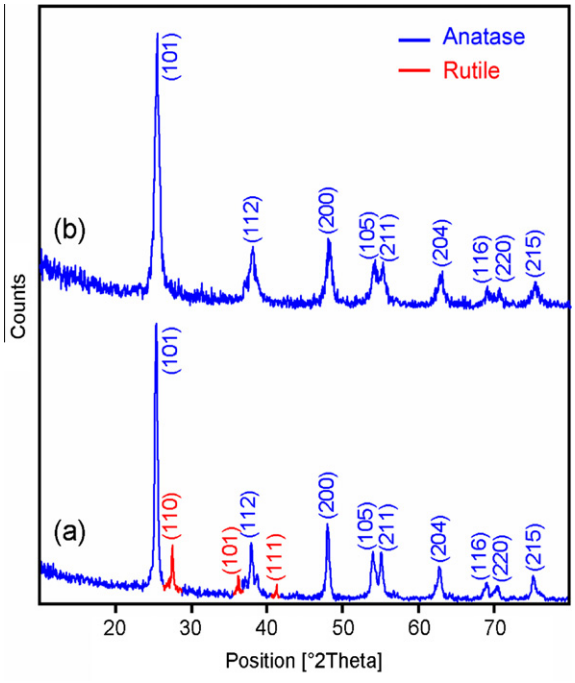

Figure 2 XRD patterns of (a) TiO_2–P25 and (b) prepared TiO_2.

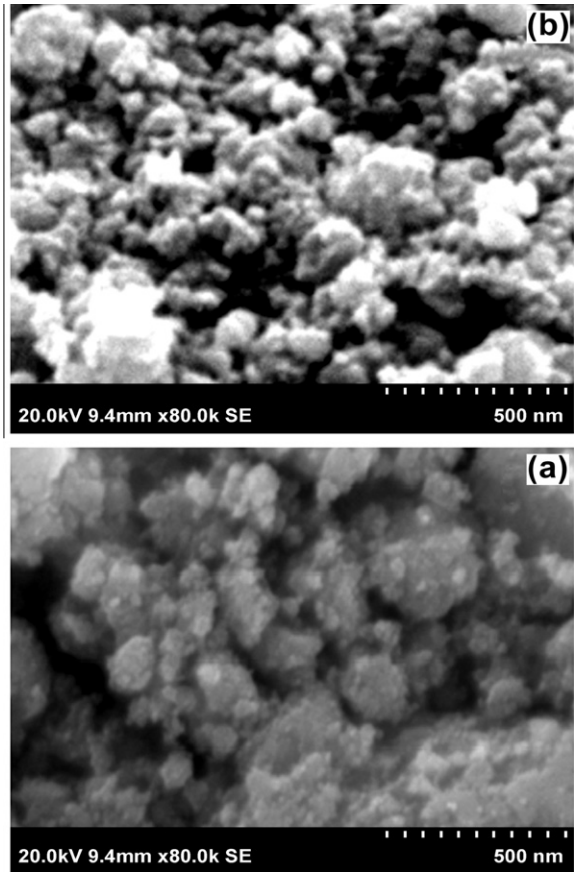

Figure 3 SEM images of (a) TiO_2–P25 and (b) prepared TiO_2.

$$D = \frac{K\lambda}{\beta \cos\theta} \quad (2)$$

where D is the crystal size of the catalyst, K is dimensionless constant, λ is the wavelength of X-ray, β is the full width at half-maximum (FWHM) of the diffraction peak and θ is the diffraction angle. The crystalline size of prepared TiO_2 is found to be 15.2 nm which is less than the size of TiO_2–P25 (30 nm).

The structure and morphology of the catalyst are very important parameters as they influence the photocatalytic activity. The SEM images of TiO_2–P25 and prepared TiO_2 are shown in Fig. 3a and b. Fig. 3a and b depict that the crystallinity is found to be more in prepared TiO_2. Fig. 4 shows the typical bright-field TEM image of the prepared TiO_2. TEM image reveals that the size of the TiO_2 nanoparticles is in the range of 10–50 nm, which is consistent with the average crystallite size (15.2 nm) estimated from XRD analysis.

In general the surface area of the catalysts is the most important factor influencing the catalytic activity. The surface area of prepared TiO_2 was determined using the nitrogen gas adsorption method. The N_2 adsorption–desorption isotherms and BET surface area plot for the synthesized sample are given in Fig. 5a and b, respectively. Fig. 5a shows the hysteresis loops of the sol–gel TiO_2, which is characteristic of the typical macroporous structures in type IV with almost vertical and nearly parallel adsorption and desorption branches. This implies that the synthesized TiO_2 sample consists of agglomerates or compacts of approximately uniform spheres. The BET surface area of prepared TiO_2 is found to be 86.5 $m^2\ g^{-1}$ which is higher than that of TiO_2–P25 (50 $m^2\ g^{-1}$). The single point adsorption total pore volume of pores less than 952.3 Å radius at P/P_o is 0.98:0.22 cm^3/g.

The diffuse reflectance spectrum of prepared TiO_2 is shown in Fig. 6. The edge absorption is slightly extended towards visible region. The band gap energy of prepared TiO_2 is found to be 3.1 eV which is equivalent to the wavelength of 397 nm.

3.2. Photodegradability of TB and RR 120

Photocatalytic degradation of Trypan Blue with TiO_2–P25 and prepared TiO_2 using solar light is shown in Fig. 7. When the dye is irradiated without catalyst there is negligible degrada-

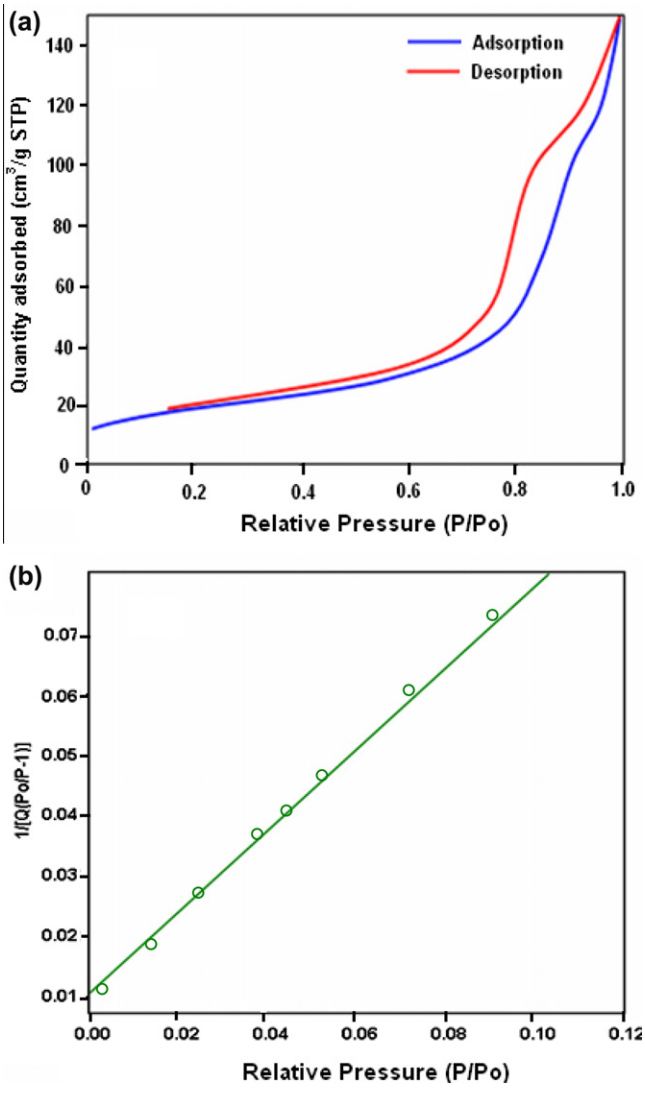

Figure 5 BET surface analysis of (a) N_2 adsorption–desorption isotherm and (b) BET surface area plot.

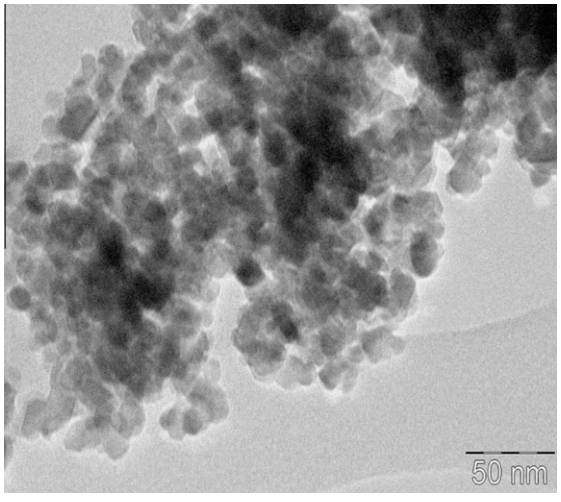

Figure 4 TEM image of prepared TiO_2.

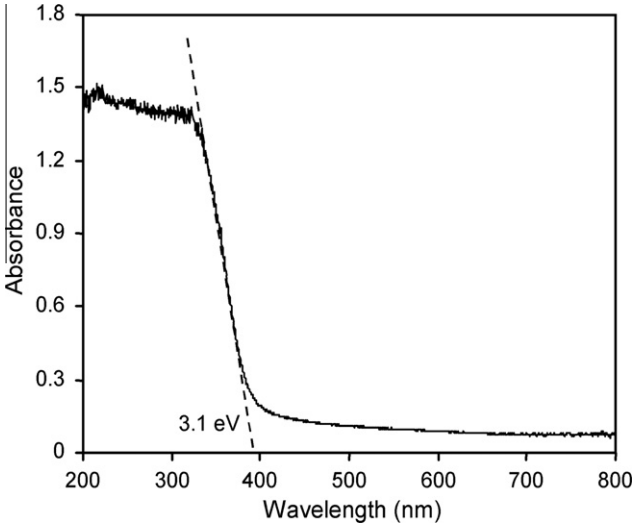

Figure 6 DRS of prepared TiO_2.

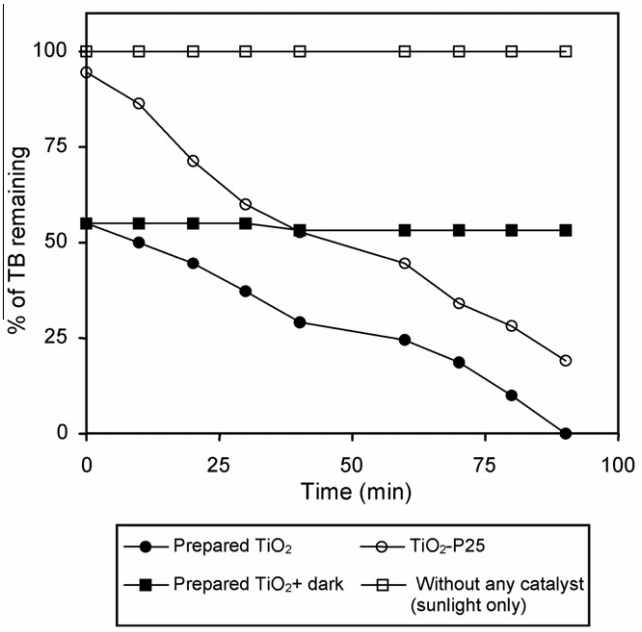

Figure 7 Photodegradability of TB; dye concentration = 1×10^{-4} mol L^{-1}, catalyst suspended = 4 g L^{-1}, pH 6.8, airflow rate = 8.1 mL s^{-1}.

tion and for the same experiment performed with the catalyst in dark 47% decrease in dye concentration occurred. This is due to adsorption of the dye on the catalyst. Dye undergoes almost complete degradation in presence of prepared TiO_2 and solar light at 90 min irradiation, whereas 81% degradation takes place at 90 min with TiO_2–P25. This shows that prepared TiO_2 process is more efficient in TB degradation than TiO_2–P25 in solar light.

The photocatalytic efficiency of this catalyst in solar light was also tested with RR 120 dye degradation. Photocatalytic degradation of RR 120 with Commercial TiO_2–P25 and prepared TiO_2 is shown in Fig. 8. When the dye is irradiated without catalyst there is negligible degradation and for the same experiment performed with the catalysts in dark, dye concentration decreases by 16.1% due to adsorption. Dye undergoes almost complete degradation with prepared TiO_2 on solar irradiation in 70 min, whereas TiO_2–P25 takes 90 min for complete degradation. This reveals the higher efficiency of prepared TiO_2 in RR 120 degradation than TiO_2–P25.

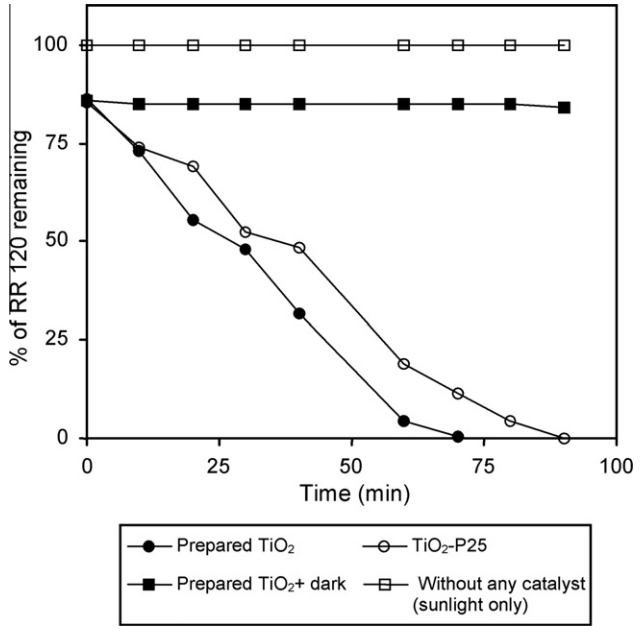

Figure 8 Photodegradability of RR 120; dye concentration = 2×10^{-4} mol L^{-1}, catalyst suspended = 4 g L^{-1}, pH 5.5, airflow rate = 8.1 mL s^{-1}.

It is seen from Fig. 7 that the initial adsorption of dye molecules in dark by prepared TiO_2 (47.0%) is higher than the adsorption by commercial TiO_2–P25 (5.5%). After complete degradation (90 min of irradiation) dye free water was obtained with prepared TiO_2. The dark adsorption and the degradation efficiency of the used TiO_2 were found to be similar to those of fresh catalyst. These observations reveal that the dye molecules adsorbed in dark underwent complete degradation during irradiation. In order to confirm the degradation of adsorbed dye molecules, FT-IR spectra of the prepared TiO_2 with the adsorbed dye (TB) molecules before and after irradiation were taken and are shown in Fig. 9b and c along with the FT-IR spectra of the fresh catalyst (Fig. 9a). Fig. 9b shows the characteristic peaks of the dye (1552 and 1501 cm^{-1} due to azo group of the dye) indicating the adsorption of dye on the catalyst. FT-IR spectrum of catalyst after irradiation, i.e., after complete degradation (Fig. 9c) reveals that the characteristic peaks of dye disappeared and spectrum in Fig. 9c is almost similar to the spectrum of fresh catalyst (Fig. 9a). This confirms that the dye molecules adsorbed on the prepared TiO_2 in dark have been completely degraded at the time of 90 min irradiation. Though TiO_2 can be excited only by UV light, dye adsorbed TiO_2 can be activated by solar light. In this case solar light excited dye molecule generates an electron, which goes to conduction band of TiO_2. This electron produces oxide ion radicals for the oxidation of dye molecules. This dye sensitized mechanism has already been reported (Kyung et al., 2005).

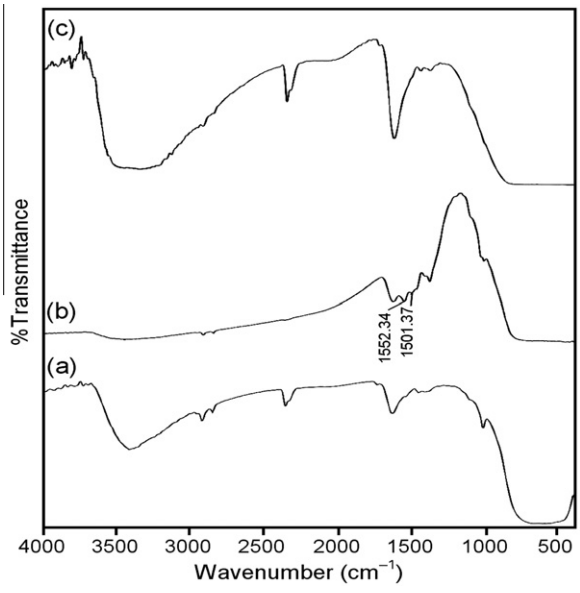

Figure 9 FT-IR spectra of (a) prepared TiO_2, (b) prepared TiO_2 after TB dye adsorption and (c) prepared TiO_2 after complete degradation of TB.

3.3. COD measurements

The mineralization of TB and RR 120 using prepared TiO_2 was also confirmed by COD measurements. The COD value of 1251.5 ppm for 1×10^{-4} mol L^{-1} of TB concentration gradually decreases to 848 ppm (67.8%) and 3.4 ppm (0.1%) after 30 and 90 min of irradiation, respectively. This indicates 99.9% mineralization of TB in 90 min.

For 2×10^{-4} mol L^{-1} of RR 120 the COD value of 2064.4 ppm gradually decreases to 1145.8 ppm (55.6%) and 102.3 ppm (4.95%) after 30 and 60 min of irradiation, respectively. This indicates 95% degradation of RR 120 in 60 min, which is almost equal to complete mineralization.

4. Conclusions

TiO_2 synthesized by sol–gel method has the anatase phase. Characterization study reveals that the size of prepared TiO_2 is 15.2 nm and its specific surface area is 86.5 $m^2 g^{-1}$. Prepared nano-TiO_2 is more efficient in the degradation of azo dyes TB and RR 120 under solar light than TiO_2–P25. Higher efficiency of prepared TiO_2 is due to its higher BET surface area than TiO_2–P25.

Acknowledgements

The authors thank the Ministry of Environment and Forests (MOEF), New Delhi, for the financial support through Research Grant No. 315-F-36, F. No. 19/9/2007-RE. One of the authors B. Krishnakumar is thankful to CSIR, New Delhi, for the award of Senior Research Fellowship. We thank Catalysis Laboratory, IIT Madras, Chennai for BET and XRD measurements. The authors also thank B. Sreedhar, IICT, Hyderabad for the TEM measurements.

References

Aarthi, T., Narahari, P., Madras, G., 2007. J. Hazard. Mater. 149, 725–734.
Collins, C.E., Incropera, F.P., Grady Jr., C.P.L., 1978. Water Res. 12, 547–584.
Huang, M.T., Miwag, T., Lu, A.Y.H., 1979. J. Biol. Chem. 254, 3935–3946.
Ince, N.H., Gonenc, D.T., 1997. Environ. Technol. 18, 179–185.
Kiwi, J., Pulgarin, C., Peringer, P., Gratzel, M., 1993. Appl. Catal. B: Environ. 3, 85–99.
Krishnakumar, B., Swaminathan, M., 2010. Indian J. Chem. Sec. A 49A, 1035–1040.
Kyung, H., Lee, J., Choi, W., 2005. Environ. Sci. Technol. 39, 2376–2382.
Luthy, R.G., Talton, J.T., 1980. Water Res. 14, 1269–1282.
Muruganandham, M., Swaminathan, M., 2006. J. Hazard. Mater. B135, 78–86.
Pagga, U., Brown, D., 1986. Chemosphere 15, 479–491.
Ravichandran, L., Selvam, K., Swaminathan, M., 2007. Aust. J. Chem. 60, 951–956.
Sobana, N., Swaminathan, M., 2007. Sep. Purif. Technol. 56, 101–107.
Tanaka, S., Ichikawa, T., 1993. Water Sci. Technol. 28, 103–110.
Toor, A.P., Verma, A., Jotshi, C.K., Bajpai, P.K., Sing, V., 2006. Dyes Pigm. 68, 53–60.
Turchi, C.S., Ollis, D.F., 1990. J. Catal. 122, 178–192.
Wang, Y., 2000. Water Res. 34, 990–994.